Coupled-Cavity Bottom-Emitting VCSELs

Presentation of Master of Science in Engineering Project

M.Sc.Eng. Student Morten Stilling

February 20th 2004

Introduction

People

Student
Morten Stilling — Odense University College of Engineering and the Southern University of Denmark

Supervisor
Ole Albrektsen — Odense University College of Engineering

Examiner
Jacob Riis Folkenberg — Crystal Fibre

About the Project

What? Optoelectronics → semiconductor lasers → VCSELs

Who? Cooperation with Odense University College of Engineering, Research Center COM at the Technical University of Denmark and Alight Technologies.

Where? Research Center COM

When? February 2003 to January 2004

Historical Context of the Project

1954 First MASER (Gordon, Zeiger and Townes)

1960 First laser (Maiman)

1962 First semiconductor lasers (four American laboratories)

1979 First VCSEL (Soda, Iga, Kitahara and Suematsu)

1990's Bloom in VCSEL research (facilitated by improvements in epitaxial growth technology)

Today VCSELs in use in local are networks ($\lambda = 850$ nm)

2004– VCSELs in use in telecommunication, optical interconnects, laser line-of-sight communication, high density optical storage, laser printing *etc.*?

Contents

- Introduction to Semiconductor Lasers, VCSELs and CCBE-VCSELs
- Theory for the Optical Field in Rotationally Symmetric Semiconductor Structures
- 3-Dimensional Model for the Optical Field in CCBE-VCSELs
- Investigation of the Optical Properties of CCBE-VCSELs
- Conclusions and Perspectives

Semiconductor Lasers

The Generic Semiconductor Laser

Optical cavity with gain section and transverse optical confinement.

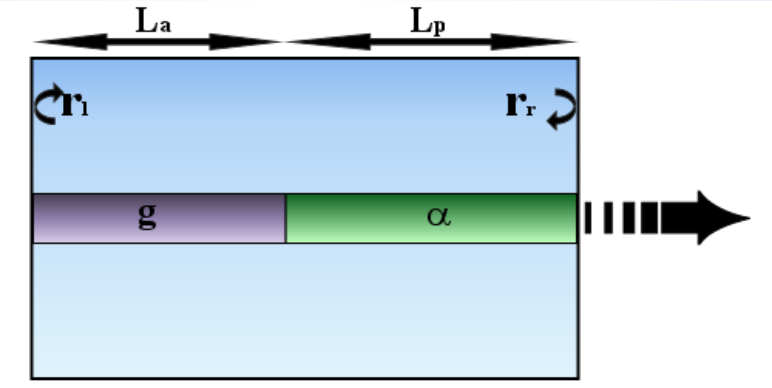

Stimulated Optical Emission in Semiconductors

Albert Einstein, 1917

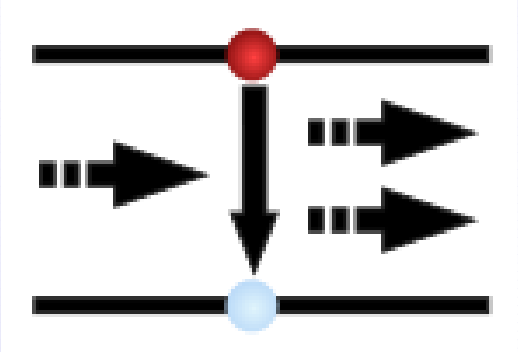

The Laser Oscillation Condition

The optical field must replicate itself upon each cavity round trip.

$$r_l \, r_r \, \mathrm{e}^{i\beta_{zp}(2L_p)} \, \mathrm{e}^{i\beta_{za}(2L_a)} = 1 \tag{1}$$

VCSELs

Vertical-Cavity Surface-Emitting Lasers

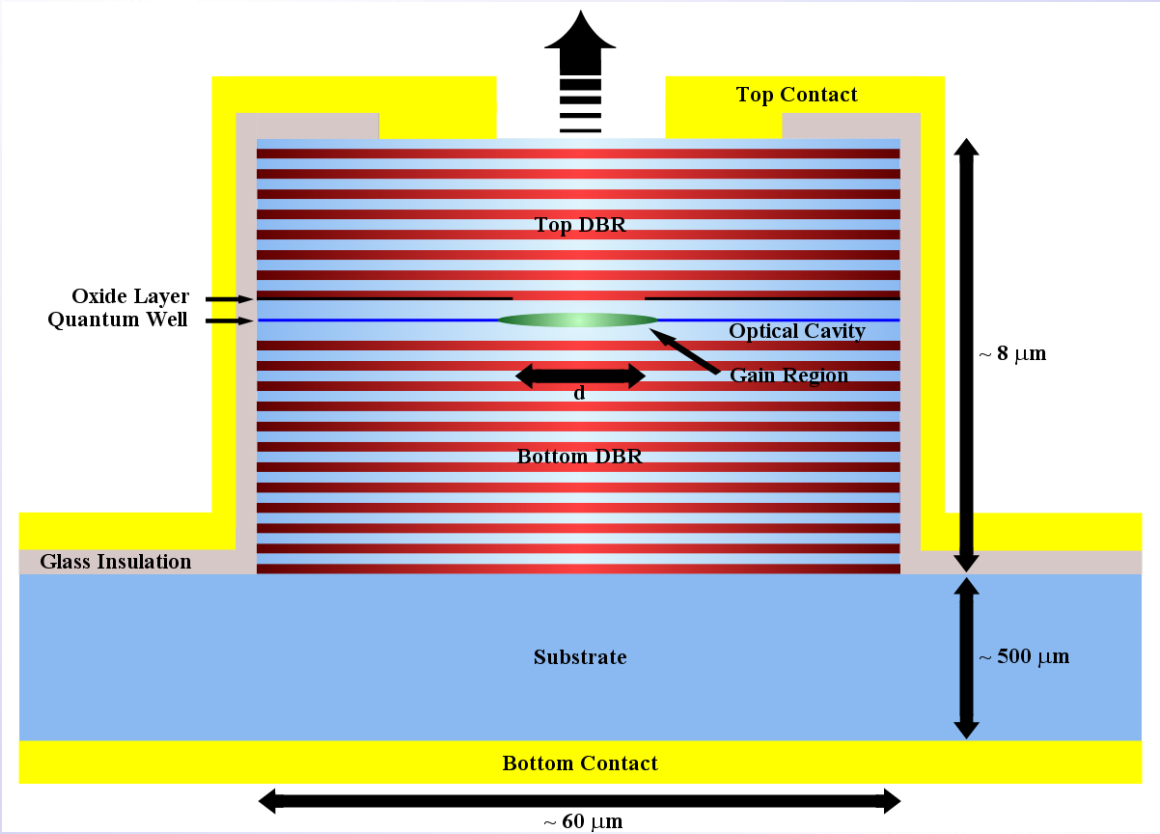
Top Contact
Top DBR
Oxide Layer
Quantum Well
Optical Cavity
Gain Region
d
~ 8 μm
Bottom DBR
Glass Insulation
Substrate
~ 500 μm
Bottom Contact
~ 60 μm

Fabrication of Oxide-Confined VCSELs

Substrate

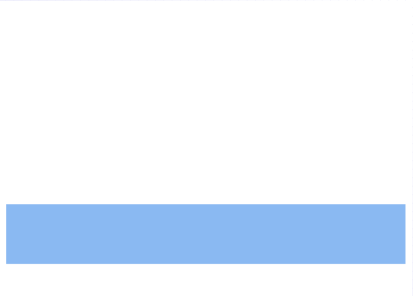

Epitaxial Growth

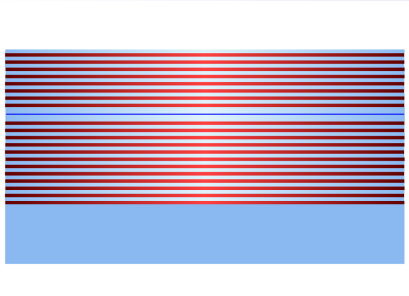

Photolithography

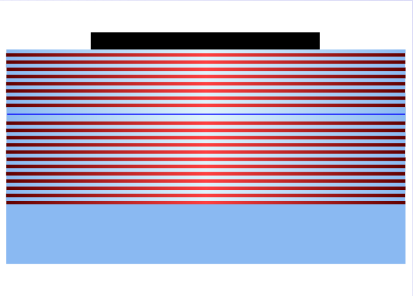

Mesa Etching

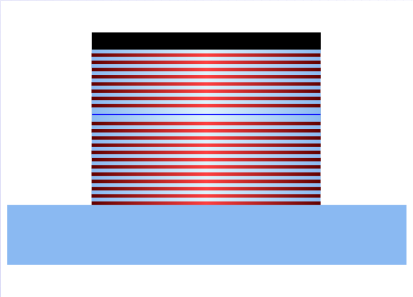

Oxidation

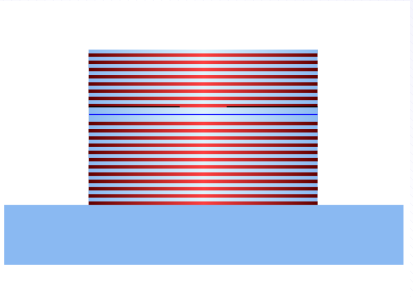

Photolithography

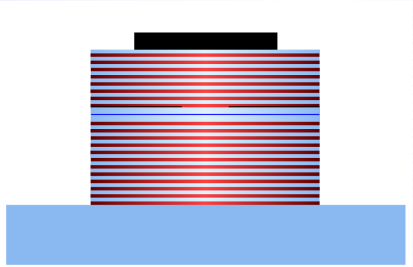

Glass Deposition

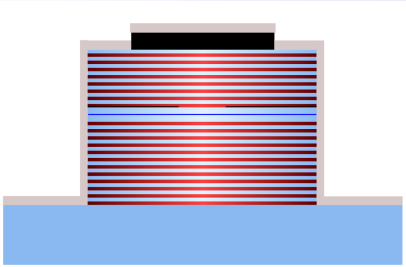

Glass Lift-Off

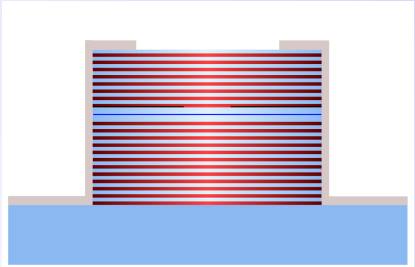

Photolithography

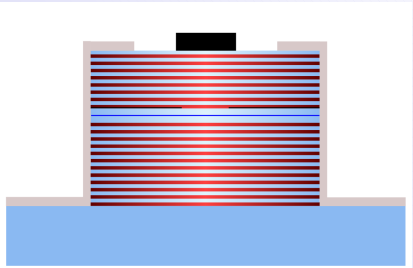

Metal Deposition

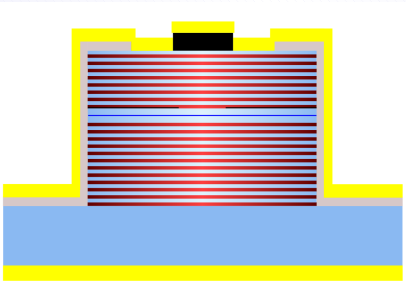

Metal Lift-Off

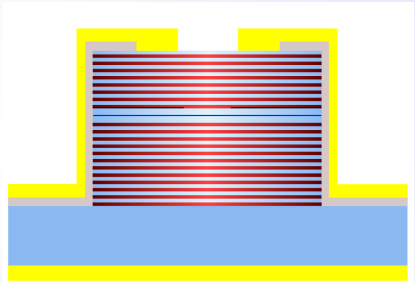

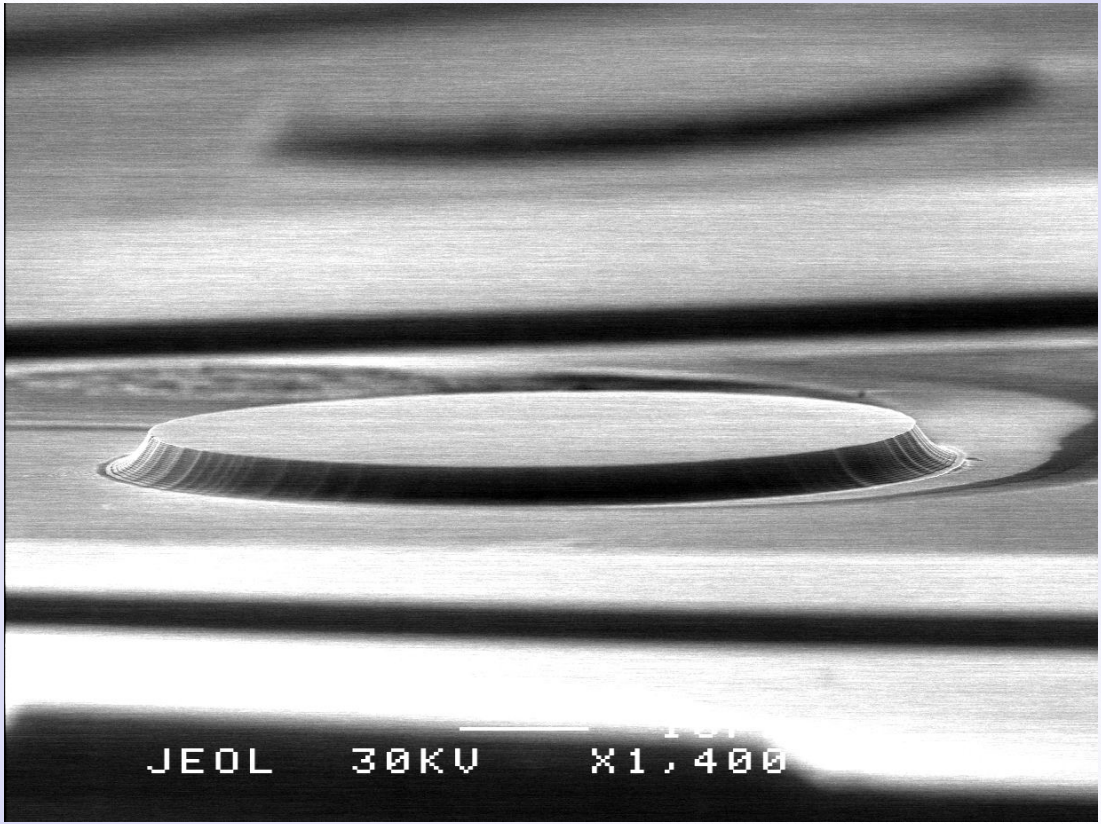
JEOL 30KV X1,400

Merits and Demerits of Oxide-Confined VCSELs

Merits:

- Rotationally symmetric output (easy coupling to *e.g.* optical fibers)
- Vertical emission (easy on-wafer testing, easy production of laser arrays, easy integration with electronics)
- Longitudinal-single-mode operation (due to short optical cavity)

Demerits:

- High optical output power *or* transverse-single-mode operation (depending on aperture size)

CCBE-VCSELs

Coupled-Cavity Bottom-Emitting
Vertical-Cavity Surface-Emitting Lasers

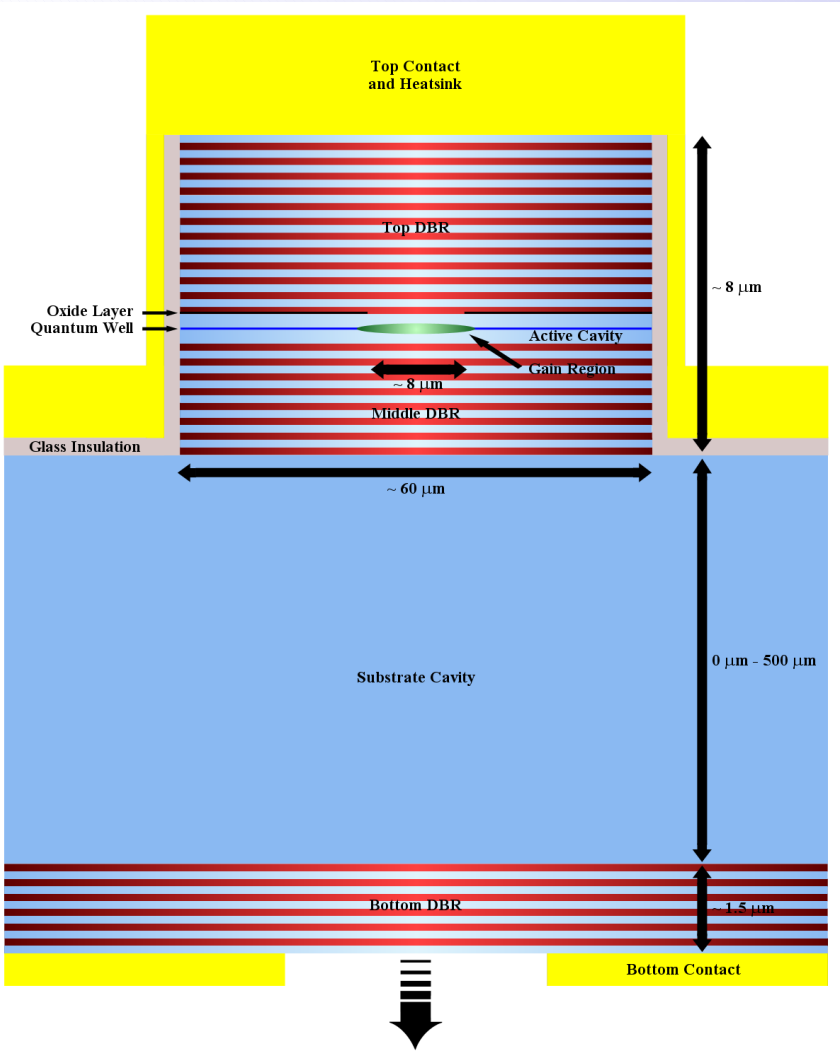
Top Contact
and Heatsink
Top DBR
~ 8 μm
Oxide Layer
Quantum Well
Active Cavity
Gain Region
~ 8 μm
Middle DBR
Glass Insulation
~ 60 μm
Substrate Cavity
0 μm - 500 μm
Bottom DBR
~ 1.5 μm
Bottom Contact

Hadley's effective index model, which is in use by Alight Technologies, is incapable of describing diffraction effects (OK in standard top-emitting VCSELs).

An eigenmode expansion model is developed.

Theory for the Optical Field in Rotationally Symmetric Semiconductor Structures

Maxwell's Equations

Maxwell's Equations:

$$\operatorname{curl}\left(\vec{\mathcal{H}}\right) = \frac{\partial \vec{\mathcal{D}}}{\partial t} + \vec{J} \tag{2}$$

$$\operatorname{curl}\left(\vec{\mathcal{E}}\right) = -\frac{\partial \vec{\mathcal{B}}}{\partial t} \tag{3}$$

$$\operatorname{div}\left(\vec{\mathcal{D}}\right) = \rho \tag{4}$$

$$\operatorname{div}\left(\vec{\mathcal{B}}\right) = 0 \tag{5}$$

Constitutive equations:

$$\vec{\mathcal{D}} = \epsilon \vec{\mathcal{E}} \tag{6}$$

$$\vec{\mathcal{B}} = \mu \vec{\mathcal{H}} \tag{7}$$

The Paraxial Wave Equation for the Optical Field

Assumptions:

- Time-independent permittivity, $\frac{\partial \epsilon}{\partial t} = 0$
- Time-independent current density, $\frac{\partial \vec{J}}{\partial t} = 0$
- Time-independent permeability, $\frac{\partial \mu}{\partial t} = 0$

Wave equation:

$$\nabla^2 \vec{\mathcal{E}} - \epsilon\mu \frac{\partial^2 \vec{\mathcal{E}}}{\partial t^2} = 0 \tag{8}$$

Paraxial wave equation:

$$\nabla^2 \mathcal{E} - \epsilon\mu \frac{\partial^2 \mathcal{E}}{\partial t^2} = 0 \tag{9}$$

The paraxial wave equation fully describes the optical field.

Helmholtz Equation for the Optical Field

Complex representation of electric field:

$$\mathcal{E}(\vec{r},t) = \mathfrak{Re}\left\{\widetilde{\mathcal{E}}(\vec{r})\,\mathrm{e}^{-i\omega t}\right\} \tag{10}$$

Helmholtz' equation:

$$\nabla^2\widetilde{\mathcal{E}}(\vec{r}) + k_0^2\widetilde{\mathcal{E}}(\vec{r}) = 0 \tag{11}$$

Using separation of variables the partial differential equation is solved.

General Solutions to Helmholtz Equation

Longitudinal part of Helmholtz' equation:

$$\frac{\mathrm{d}^2\widetilde{\mathcal{E}}_z(z)}{\mathrm{d}z^2} + \beta_z^2\widetilde{\mathcal{E}}_z(z) = 0 \tag{12}$$

Solutions to longitudinal part:

$$\widetilde{\mathcal{E}}_z(z) = C_1\,\mathrm{e}^{i\beta_z z} + C_2\,\mathrm{e}^{-i\beta_z z} \tag{13}$$

Solutions describe the propagation of the field towards $\pm z$.

Azimuthal part of Helmholtz' equation:

$$\frac{\mathrm{d}^2\widetilde{\mathcal{E}}_\theta(\theta)}{\mathrm{d}\theta^2} + m^2\widetilde{\mathcal{E}}_\theta(\theta) = 0 \tag{14}$$

Solutions to azimuthal part:

$$\widetilde{\mathcal{E}}_\theta(\theta) = C_3 \cos(m\theta) \tag{15}$$

with $m = 0, 1, 2, 3, \cdots$.

Sine-solutions are neglected since they constitute a degenerate orthogonal set of solutions due to the rotational symmetry.

Radial part of Helmholtz' equation:

$$r^2 \frac{\mathrm{d}^2 \widetilde{\mathcal{E}}_r(r)}{\mathrm{d}r^2} + r \frac{\mathrm{d}\widetilde{\mathcal{E}}_r(r)}{\mathrm{d}r} + \left[\beta_r^2 r^2 - m^2\right] \widetilde{\mathcal{E}}_r(r) = 0, \tag{16}$$

Solutions to radial part:

$$\widetilde{\mathcal{E}}_r(r) = C_4 \, \mathrm{J}_m(\beta_r r) \tag{17}$$

Solutions consisting of Bessel functions of the second kind are non-physical and are neglected.

3-Dimensional Model for the Optical Field in CCBE-VCSELs

Model Overview

1. For a given wavelength Maxwells equations are solved to find a complete orthogonal set of eigenfunctions (the basic eigenmodes) for a reference cylinder with totally reflecting walls.
2. The optical field in each epitaxial layer is expanded in terms of the basic eigenmodes, the expansions are inserted into Maxwells equations and the eigenvalue problems that arise are solved for the eigenfunctions (the layer eigenmodes) of each layer.
3. The optical fields in all epitaxial layers are expanded in terms of the respective layer eigenmodes and the reflection- and transmission coefficients for all layer eigenmodes at all interfaces between epitaxial layers are found.
4. An eigenvalue problem is set up and the wavelength and gain are varied to find eigenfunctions with eigenvalue 1.

The Basic Eigenmodes

Reference cylinder with perfectly reflecting walls.

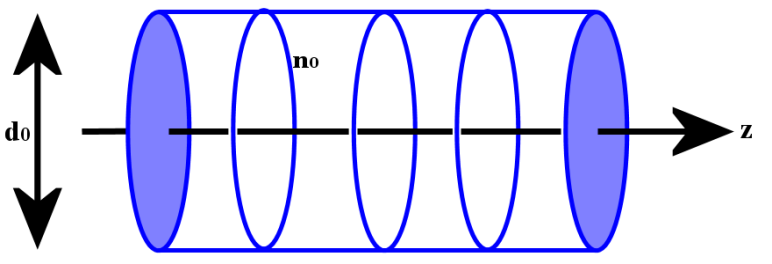

Transverse solutions in cylinder:

$$\widetilde{\mathcal{E}}_t(r,\theta) = C\,\mathrm{J}_m(\beta_r r)\,\cos(m\theta) \tag{18}$$

The transverse solutions combined with corresponding longitudinal solutions are denoted the *basic eigenmodes*, $|\widetilde{\mathcal{E}}_{0i}>$.

Basis set consisting of the first 12 basic eigenmodes, $N = 12$.

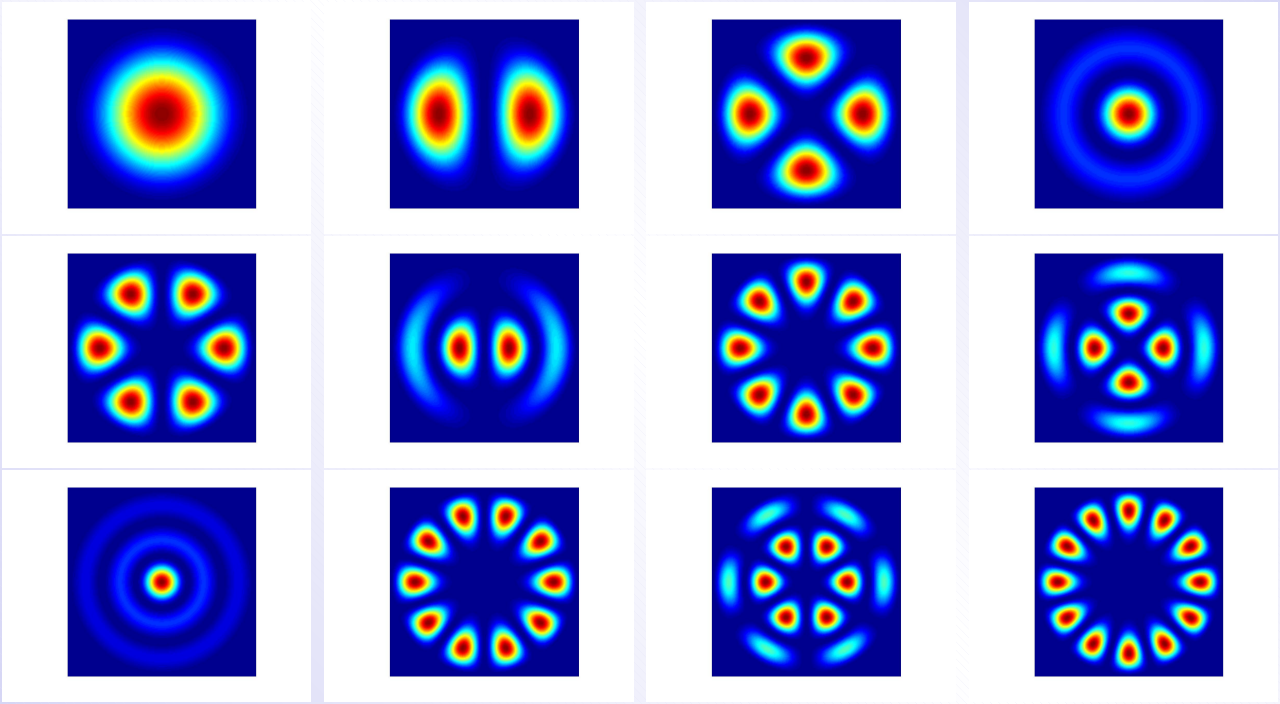

The Layer Eigenmodes

The radial part of Helmholtz' equation as an eigenvalue equation:

$$\hat{\mathrm{O}}_m \,|\widetilde{\mathcal{E}}_m> = \beta_{zm}^2 \,|\widetilde{\mathcal{E}}_m> \tag{19}$$

The operator is split into two.

$$\hat{\mathrm{O}}_m = \hat{\mathrm{O}}_0 + \hat{\mathrm{O}}_m' \tag{20}$$

The layer eigenmodes are expanded in terms of the basic eigenmodes:

$$|\widetilde{\mathcal{E}}_{m,k}> = \sum_{i=1}^{N} a_{ki} \,|\widetilde{\mathcal{E}}_{0i}> \tag{21}$$

The coefficients in the expansion are found by solving the eigenvalue equation (an $N \times N$ matrix eigenvalue equation).

The Reflection Properties of the "Mirrors"

Interface transmission matrices $(2N \times 2N)$ are set up for all interfaces.

Transmission line transmission matrices $(2N \times 2N)$ are set up for all transmission lines.

The total reflection- and transmission properties of the structure on either side of the active cavity are found by multiplying the transmission matrices in the appropriate order.

The Eigenvalue Problem

$N \times N$ reflection matrices are extracted from the transmission matrices of the top- and bottom "mirrors".

A matrix eigenvalue equation, representing the laser oscillation condition, is set up:

$$\left[\bar{\mathrm{R}}_t \, \bar{\mathrm{T}}_c \, \bar{\mathrm{R}}_b \, \bar{\mathrm{T}}_c\right] \, \widetilde{\mathcal{E}} = \bar{\mathrm{I}} \, \widetilde{\mathcal{E}} \tag{22}$$

Eigenfunctions with eigenvalue 1 are laser eigenmodes.

Test of 3-Dimensional Optical Model

The Benchmark VCSEL Structure

From the article *Comparison of optical VCSEL Models on the Simulation of Oxide-Confined Devices* by Peter Bienstman *et al.*

Layer(s)	**Thickness**	**Material**	**Refractive Index**
Ambience	-	Air	1
Top DBR	69.49 nm	GaAs	3.53
(24.5 periods)	79.63 nm	AlGaAs	3.08
Buffer	63.71 nm − x	AlGaAs	3.08
Aperture	15.93 nm	AlAs	2.95 for $r < d/2$
		AlOx	1.60 for $r > d/2$
Buffer	x	AlGaAs	3.08
Cavity	136.49 nm	GaAs	3.53
	5.00 nm	QW	3.53
	136.49 nm	GaAs	3.53
Bottom DBR	79.63 nm	AlGaAs	3.08
(29.5 periods)	69.49 nm	GaAs	3.53
Substrate	-	GaAs	3.53

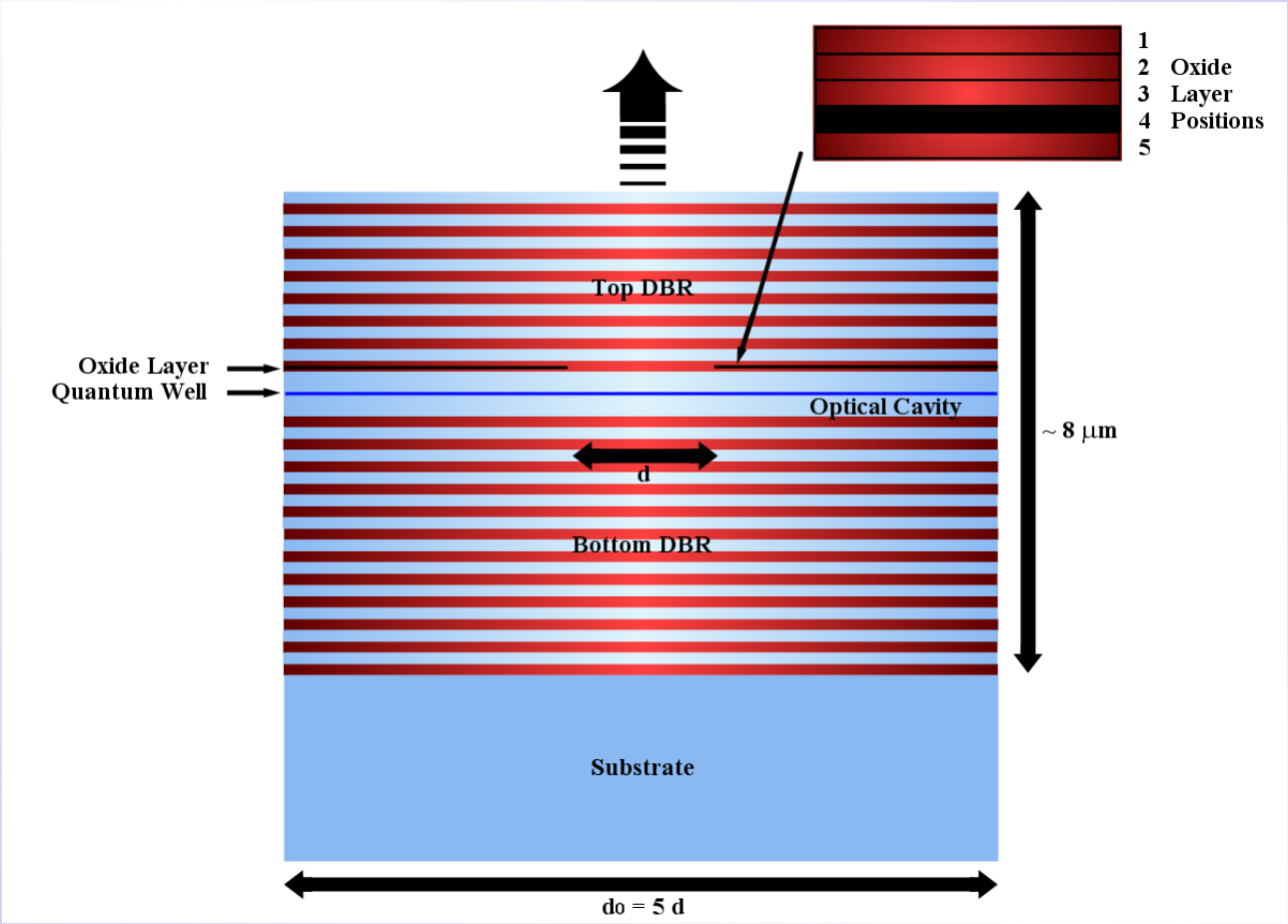
1
2 Oxide
3 Layer
4 Positions
5
Top DBR
Oxide Layer
Quantum Well
Optical Cavity
~ 8 μm
d
Bottom DBR
Substrate
do = 5 d

Convergence Analysis

The benchmark VCSEL with an 8 μm and a 1 μm antinode aperture is analyzed using 10 to 120 basic eigenmodes.

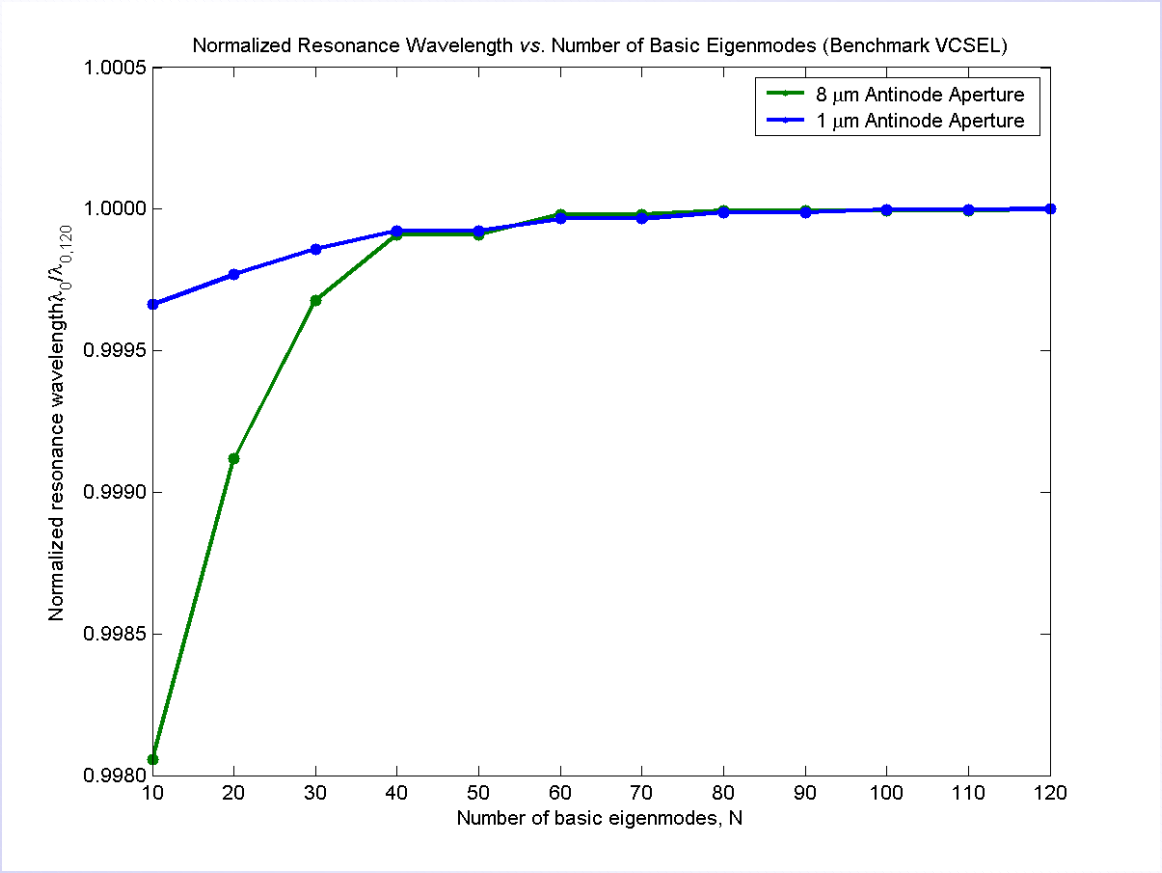
Normalized Resonance Wavelength vs. Number of Basic Eigenmodes (Benchmark VCSEL)
8 μm Antinode Aperture
1 μm Antinode Aperture
Normalized resonance wavelength $\hat{\lambda}_0/\hat{\lambda}_{0,120}$
Number of basic eigenmodes, N
1.0005
1.0000
0.9995
0.9990
0.9985
0.9980
10
20
30
40
50
60
70
80
90
100
110
120

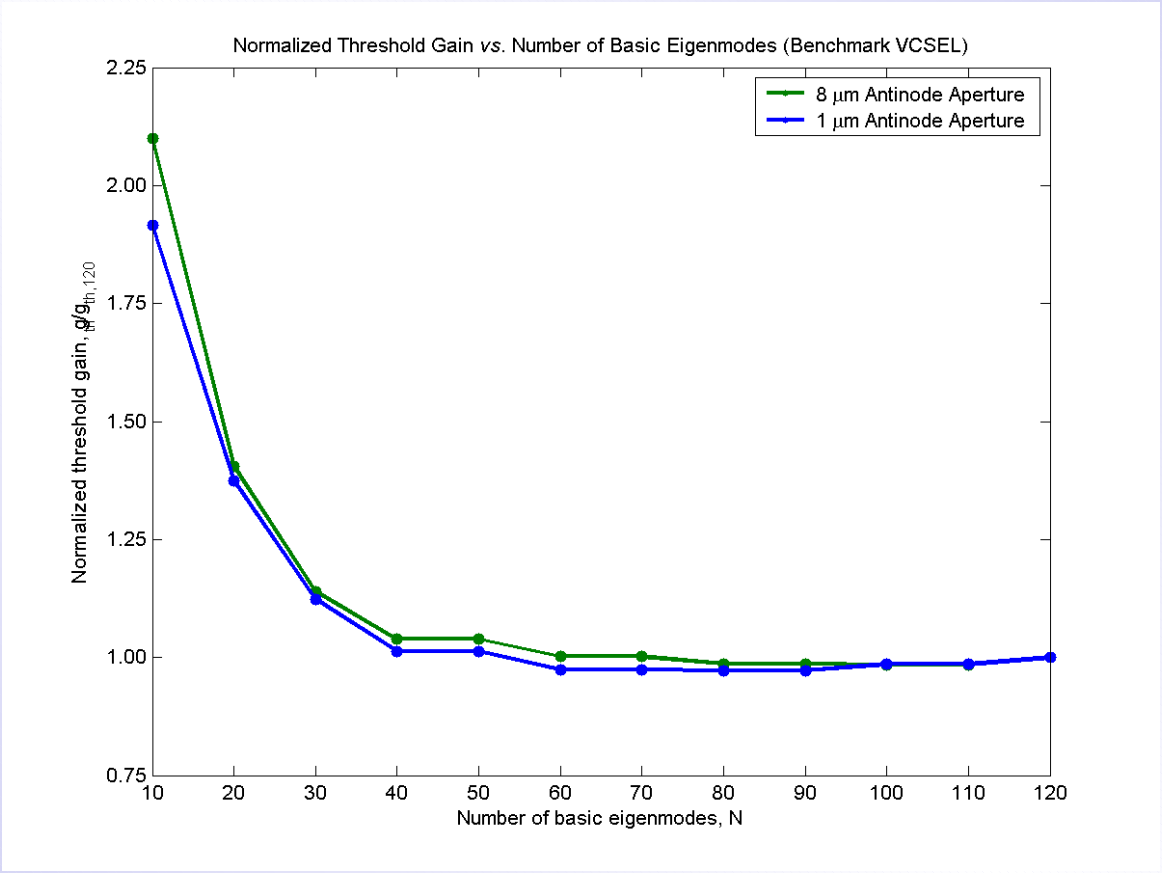
Normalized Threshold Gain vs. Number of Basic Eigenmodes (Benchmark VCSEL)
8 μm Antinode Aperture
1 μm Antinode Aperture
Normalized threshold gain, $g/g_{th,120}$
Number of basic eigenmodes, N
2.25
2.00
1.75
1.50
1.25
1.00
0.75
10
20
30
40
50
60
70
80
90
100
110
120

Estimated "accuracy" when using 120 basic eigenmodes:

- Resonance wavelengths: $\Delta\lambda \approx \pm 0.01$ %
- Threshold gains: $\Delta g_{th} \approx \pm 3$ %

Analysis of the Benchmark VCSEL Structure

Eight different analyses are performed.

Results are compared to those found using the 11 different models of the article.

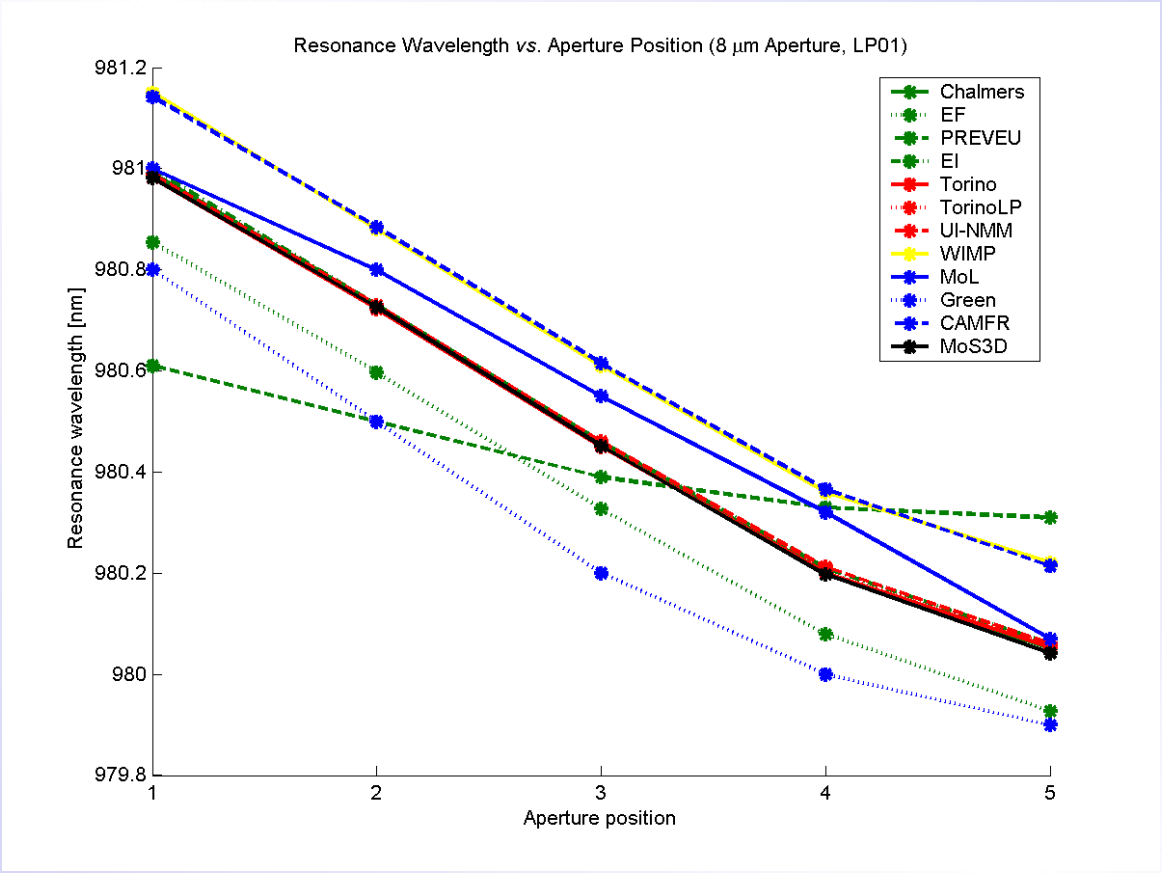
Resonance Wavelength vs. Aperture Position (8 μm Aperture, LP01)
Resonance wavelength [nm]
Aperture position
981.2
981
980.8
980.6
980.4
980.2
980
979.8
1
2
3
4
5
Chalmers
EF
PREVEU
EI
Torino
TorinoLP
UI-NMM
WIMP
MoL
Green
CAMFR
MoS3D

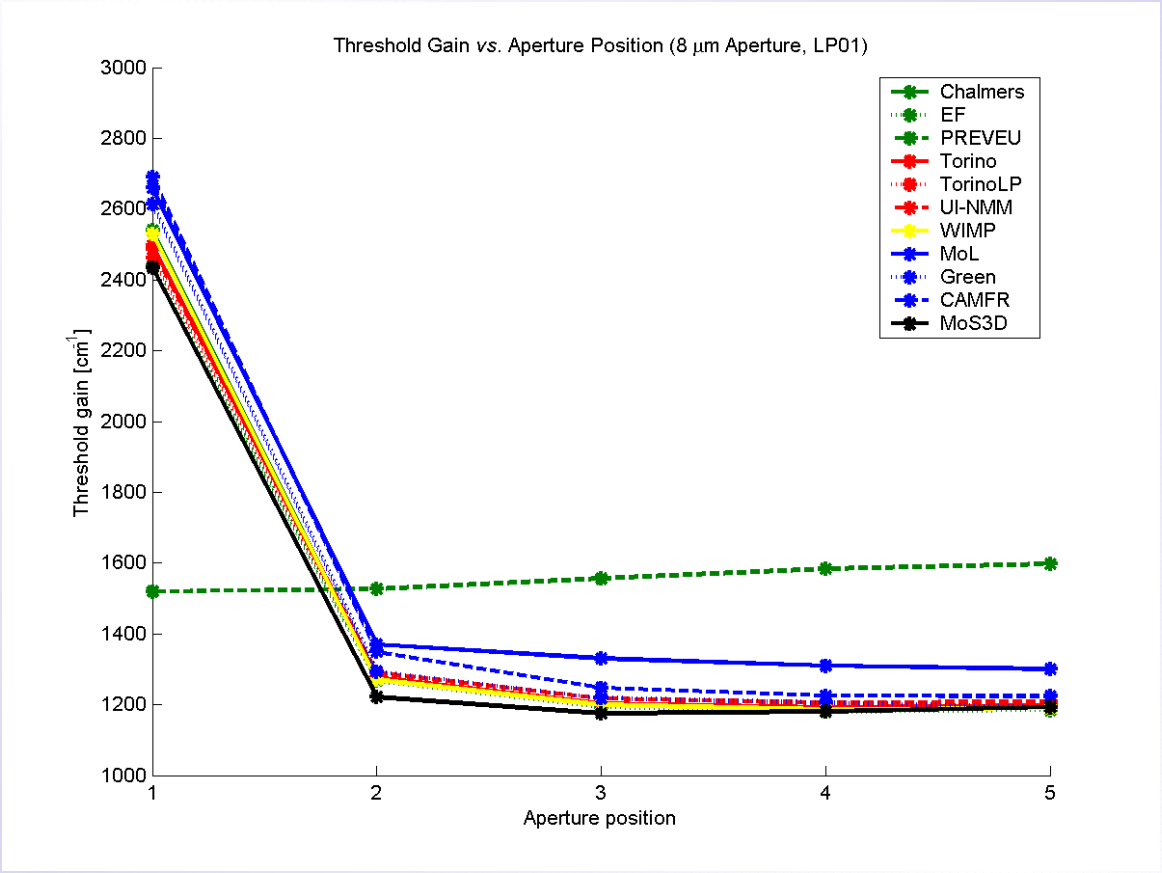
Threshold Gain vs. Aperture Position (8 μm Aperture, LP01)
Threshold gain [cm-1]
Aperture position
3000
2800
2600
2400
2200
2000
1800
1600
1400
1200
1000
1
2
3
4
5
Chalmers
EF
PREVEU
Torino
TorinoLP
UI-NMM
WIMP
MoL
Green
CAMFR
MoS3D

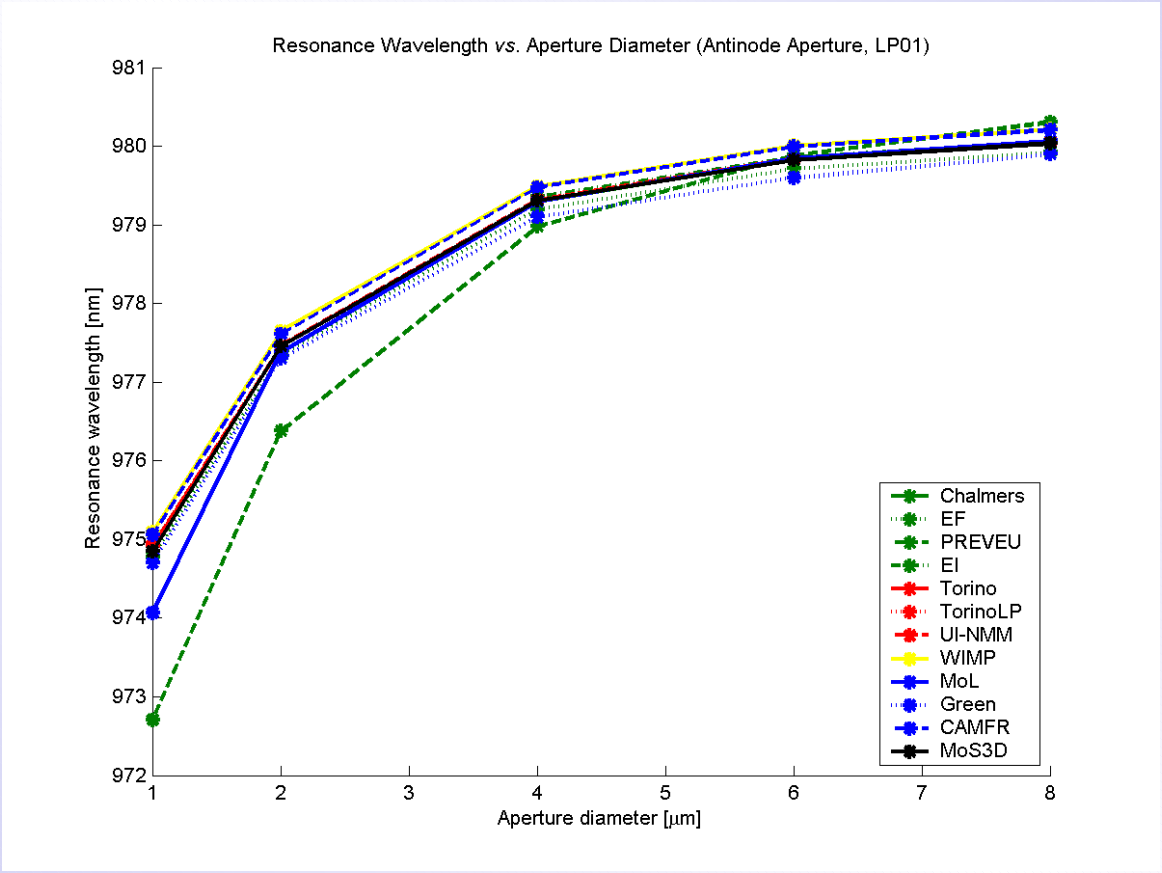
Resonance Wavelength vs. Aperture Diameter (Antinode Aperture, LP01)
Resonance wavelength [nm]
Aperture diameter [μm]
981
980
979
978
977
976
975
974
973
972
1
2
3
4
5
6
7
8
Chalmers
EF
PREVEU
EI
Torino
TorinoLP
UI-NMM
WIMP
MoL
Green
CAMFR
MoS3D

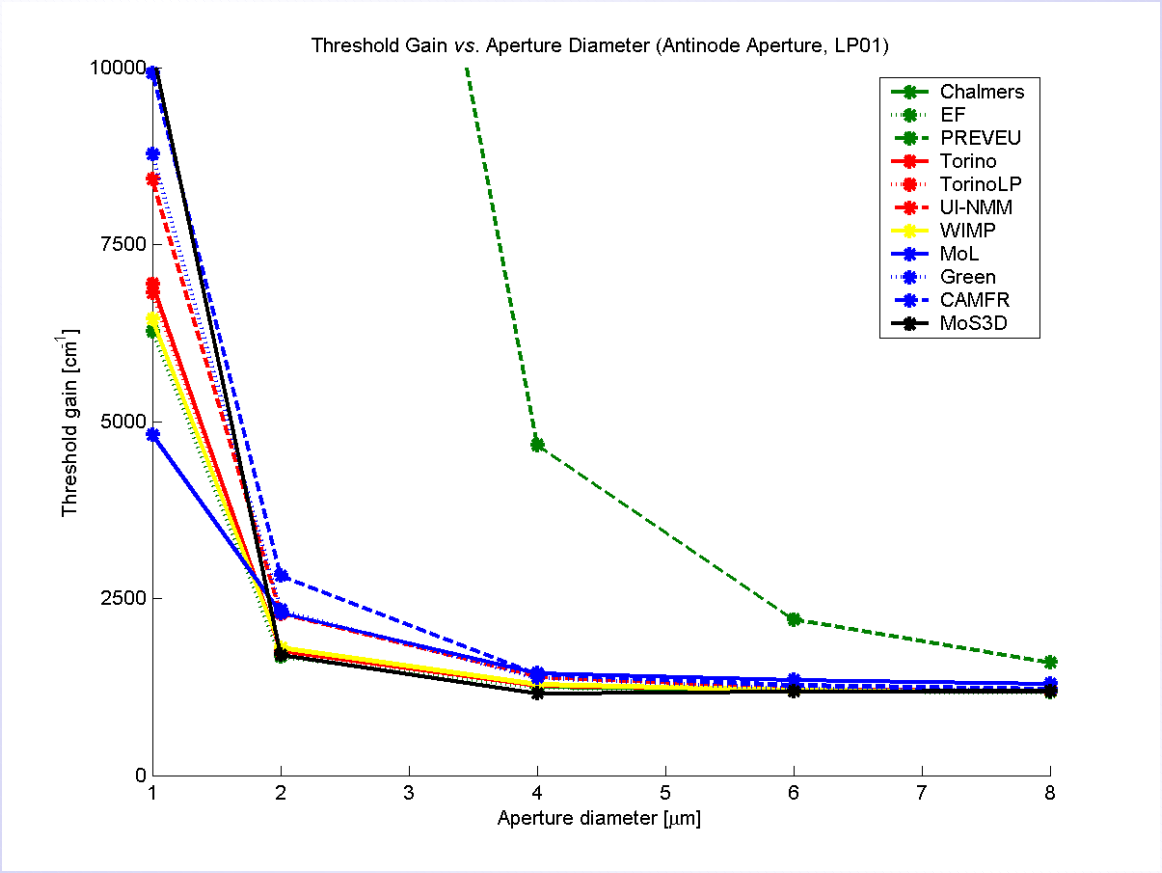
Threshold Gain vs. Aperture Diameter (Antinode Aperture, LP01)
Threshold gain [cm^{-1}]
Aperture diameter [μm]
10000
7500
5000
2500
0
1
2
3
4
5
6
7
8
Chalmers
EF
PREVEU
Torino
TorinoLP
UI-NMM
WIMP
MoL
Green
CAMFR
MoS3D

Conclusions of Tests

Correspondence between the results for the resonance wavelengths:

- Qualitative correspondence: MoS3D is around average
- Quantitative correspondence: Other models lie within $\pm 0.03\%$

Correspondence between the results for the threshold gains:

- Qualitative correspondence: MoS3D is below other models
- Quantitative correspondence: Other models lie within $\pm 10\%$

Investigation of the Optical Properties of CCBE-VCSELs

The Benchmark CCBE-VCSEL Structure

Extended benchmark VCSEL structure with

- Number of periods in top DBR: 33.5
- Antinode aperture: $d = 8\ \mu$m
- Substrate cavity length: $0\ \mu\text{m} \leq \text{L} \leq 500\ \mu\text{m}$
- Number of periods in middle- and bottom DBR: $N_1 + N_2 = 24.5$

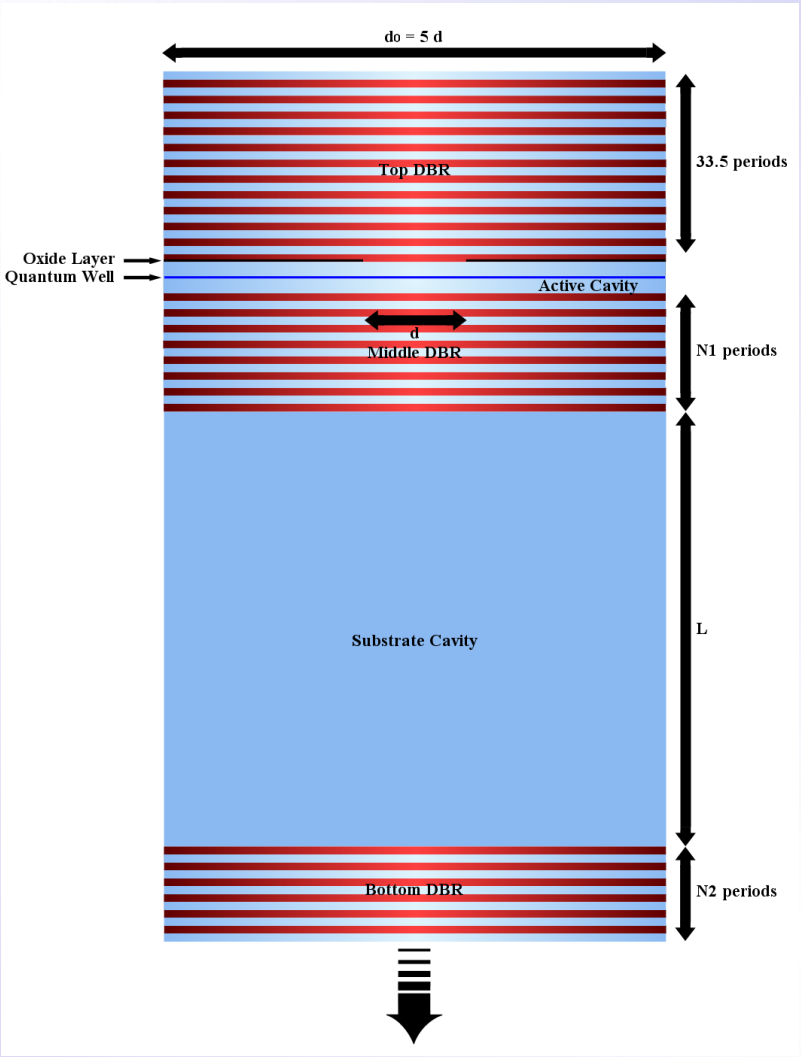
do = 5 d
Top DBR
33.5 periods
Oxide Layer
Quantum Well
Active Cavity
d
Middle DBR
N1 periods
Substrate Cavity
L
Bottom DBR
N2 periods

1-Dimensional Analysis of the Benchmark CCBE-VCSEL Structure

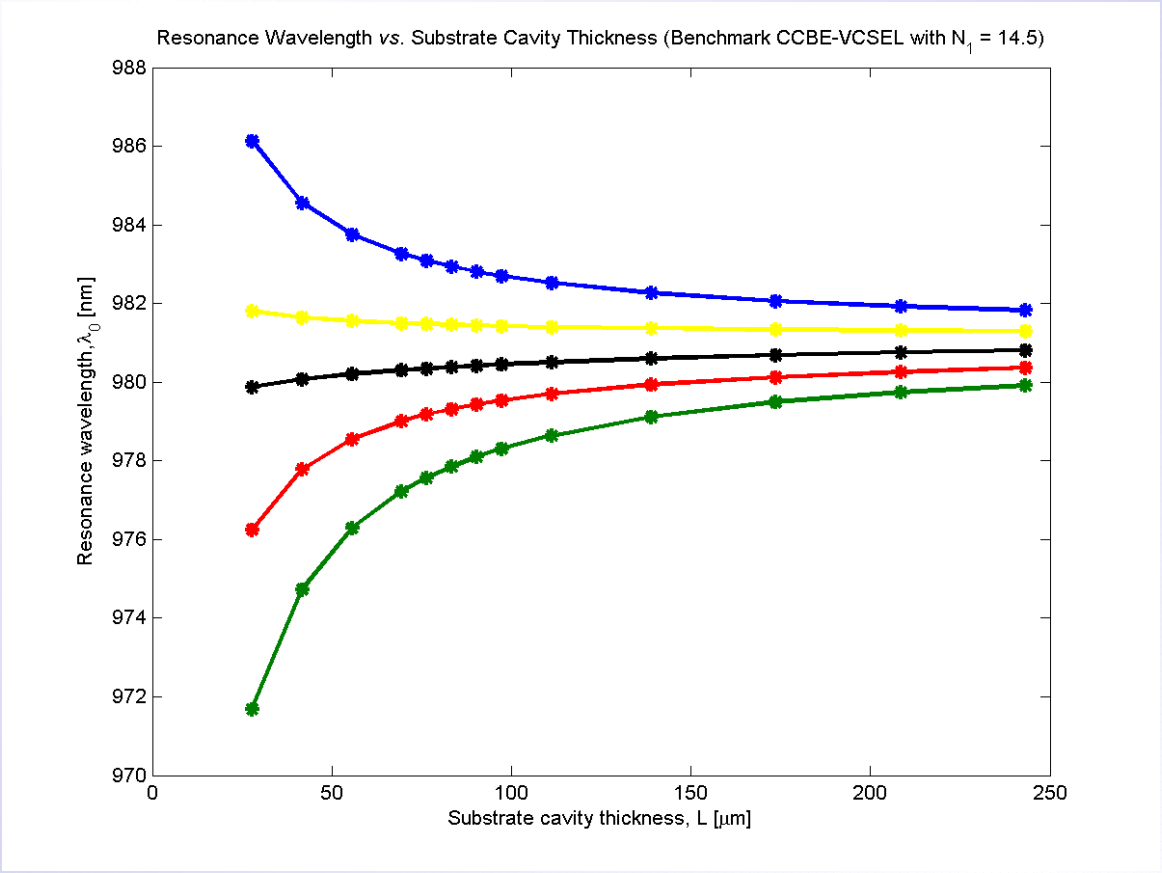
Resonance Wavelength *vs.* Substrate Cavity Thickness (Benchmark CCBE-VCSEL with N_1 = 14.5)
Resonance wavelength, λ_0 [nm]
988
986
984
982
980
978
976
974
972
970
0
50
100
150
200
250
Substrate cavity thickness, L [μm]

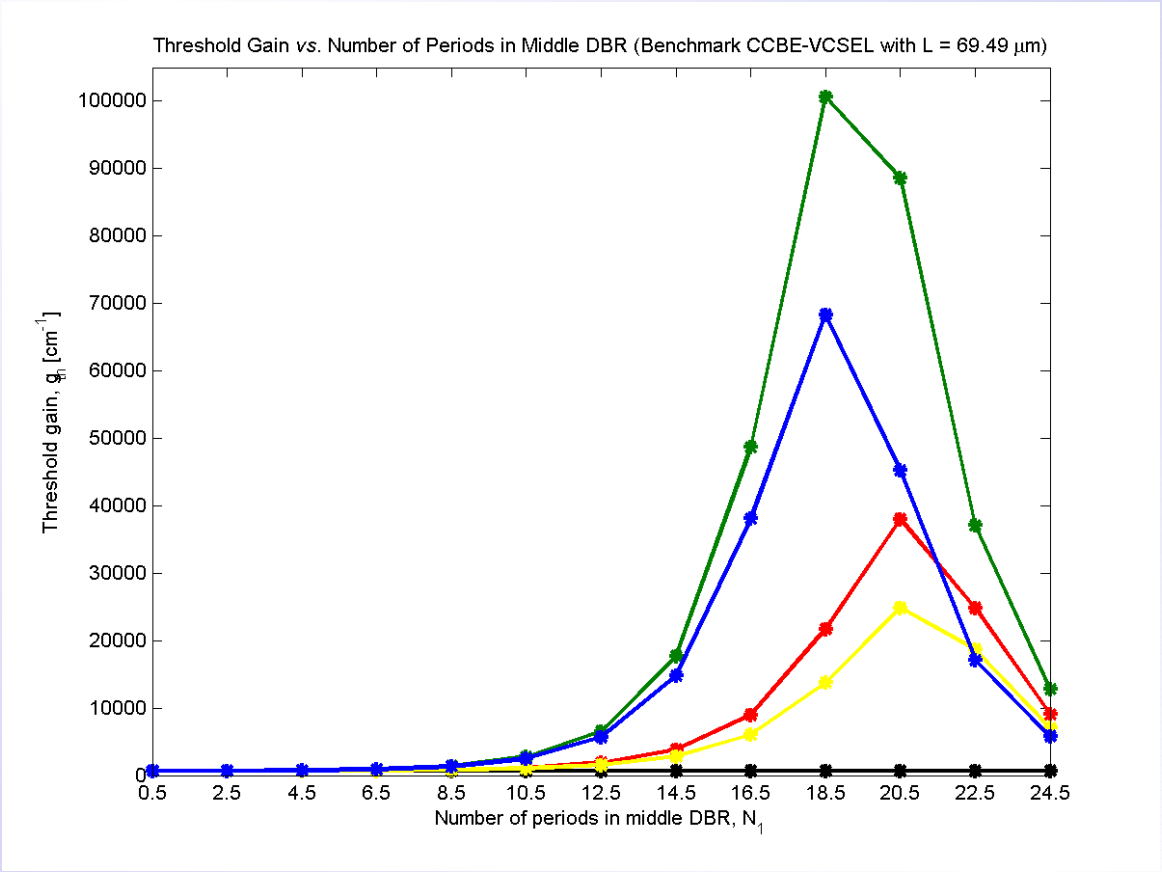
Threshold Gain vs. Number of Periods in Middle DBR (Benchmark CCBE-VCSEL with L = 69.49 μm)
Threshold gain, g_{th} [cm^{-1}]
100000
90000
80000
70000
60000
50000
40000
30000
20000
10000
0
0.5
2.5
4.5
6.5
8.5
10.5
12.5
14.5
16.5
18.5
20.5
22.5
24.5
Number of periods in middle DBR, N_1

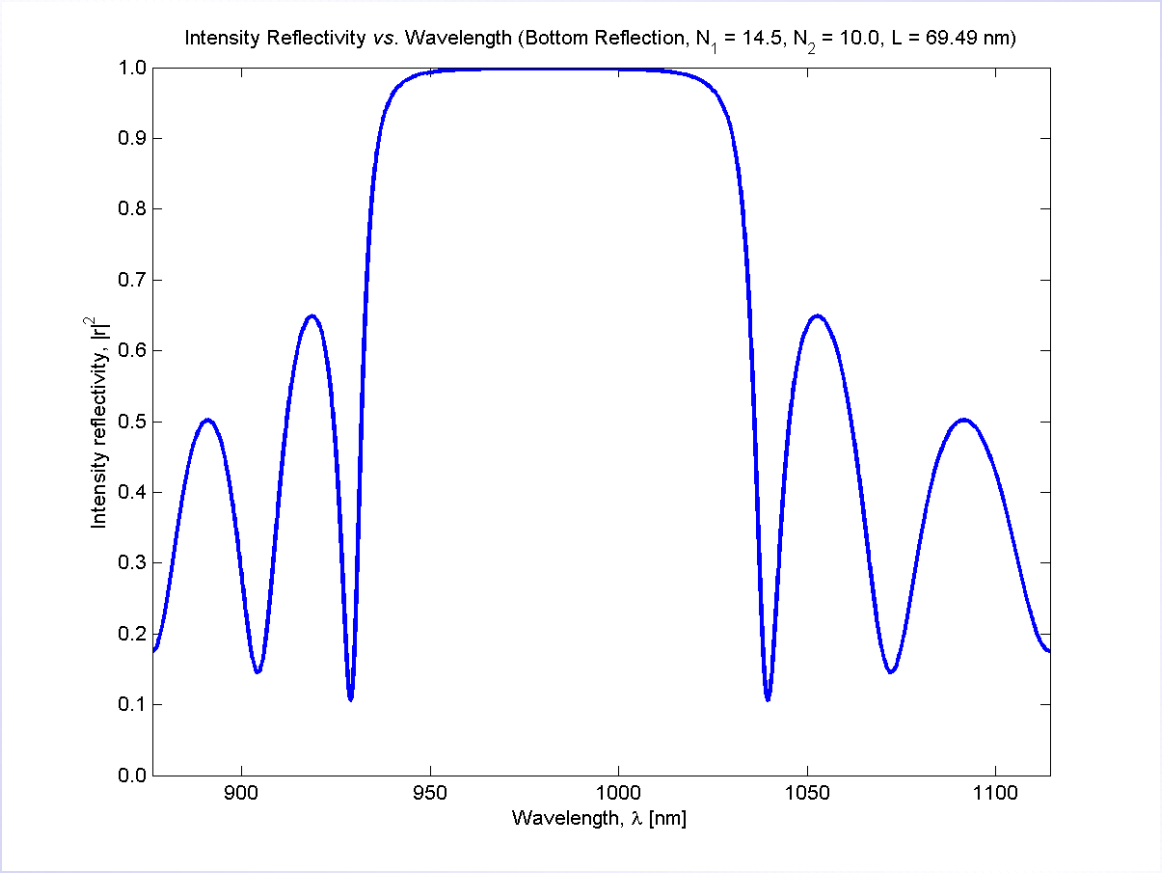
Intensity Reflectivity *vs.* Wavelength (Bottom Reflection, N_1 = 14.5, N_2 = 10.0, L = 69.49 nm)
Intensity reflectivity, $|r|^2$
1.0
0.9
0.8
0.7
0.6
0.5
0.4
0.3
0.2
0.1
0.0
900
950
1000
1050
1100
Wavelength, λ [nm]

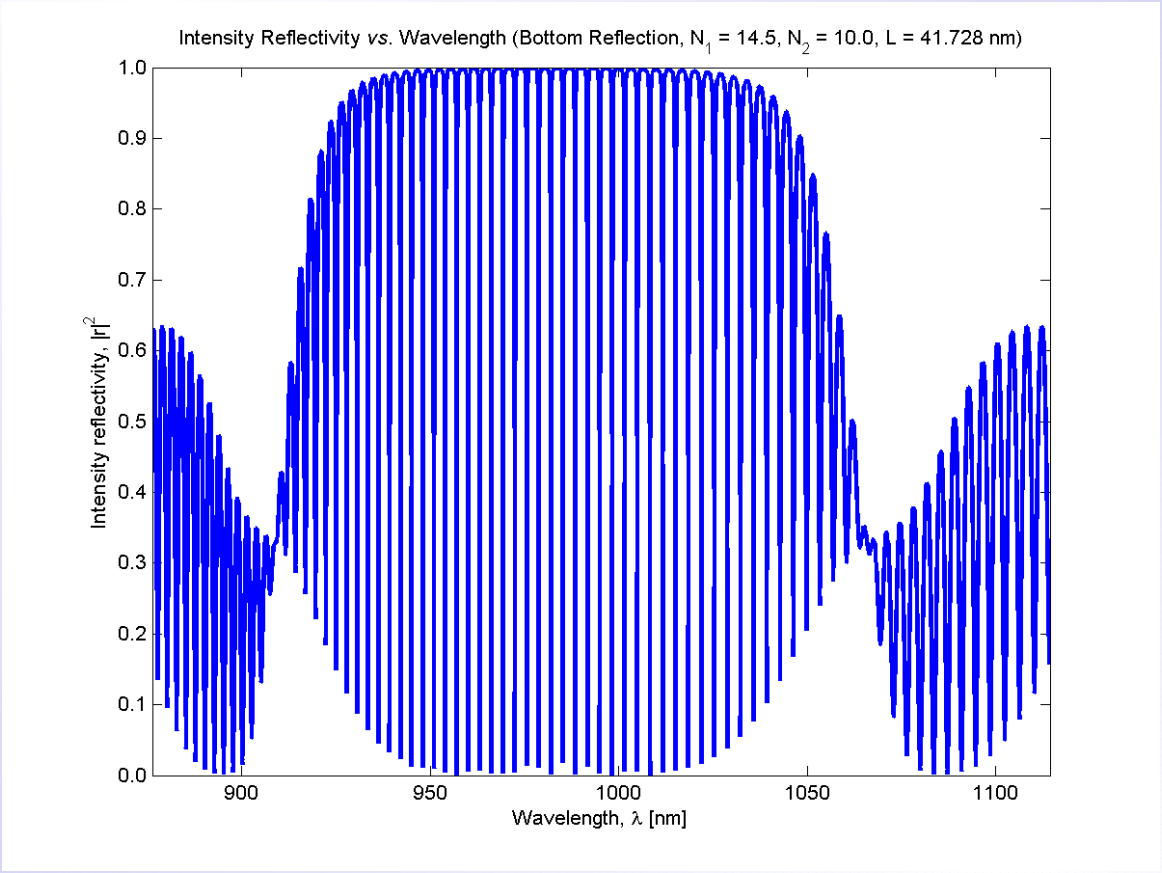
Intensity Reflectivity vs. Wavelength (Bottom Reflection, N1 = 14.5, N2 = 10.0, L = 41.728 nm)
Intensity reflectivity, |r|2
1.0
0.9
0.8
0.7
0.6
0.5
0.4
0.3
0.2
0.1
0.0
900
950
1000
1050
1100
Wavelength, λ [nm]

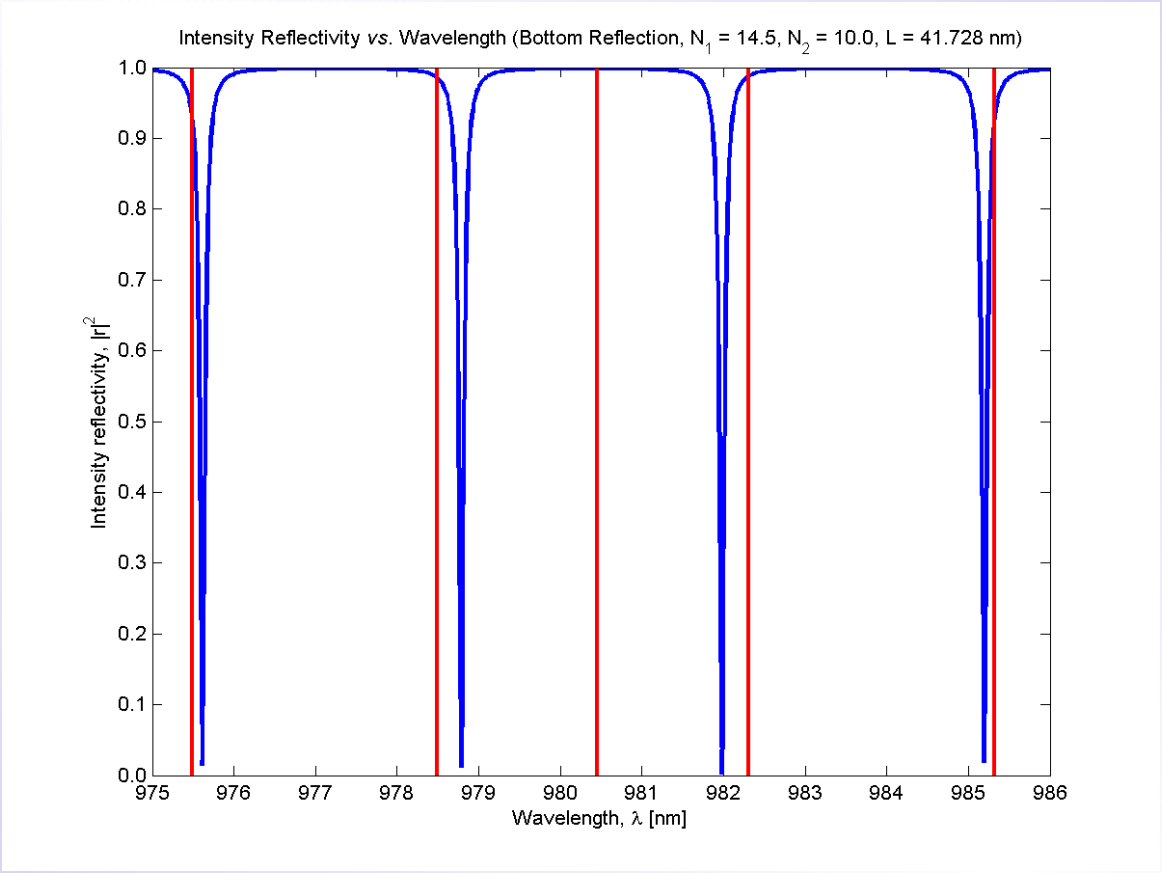
Intensity Reflectivity vs. Wavelength (Bottom Reflection, N1 = 14.5, N2 = 10.0, L = 41.728 nm)
Intensity reflectivity, |r|2
Wavelength, λ [nm]
1.0
0.9
0.8
0.7
0.6
0.5
0.4
0.3
0.2
0.1
0.0
975
976
977
978
979
980
981
982
983
984
985
986

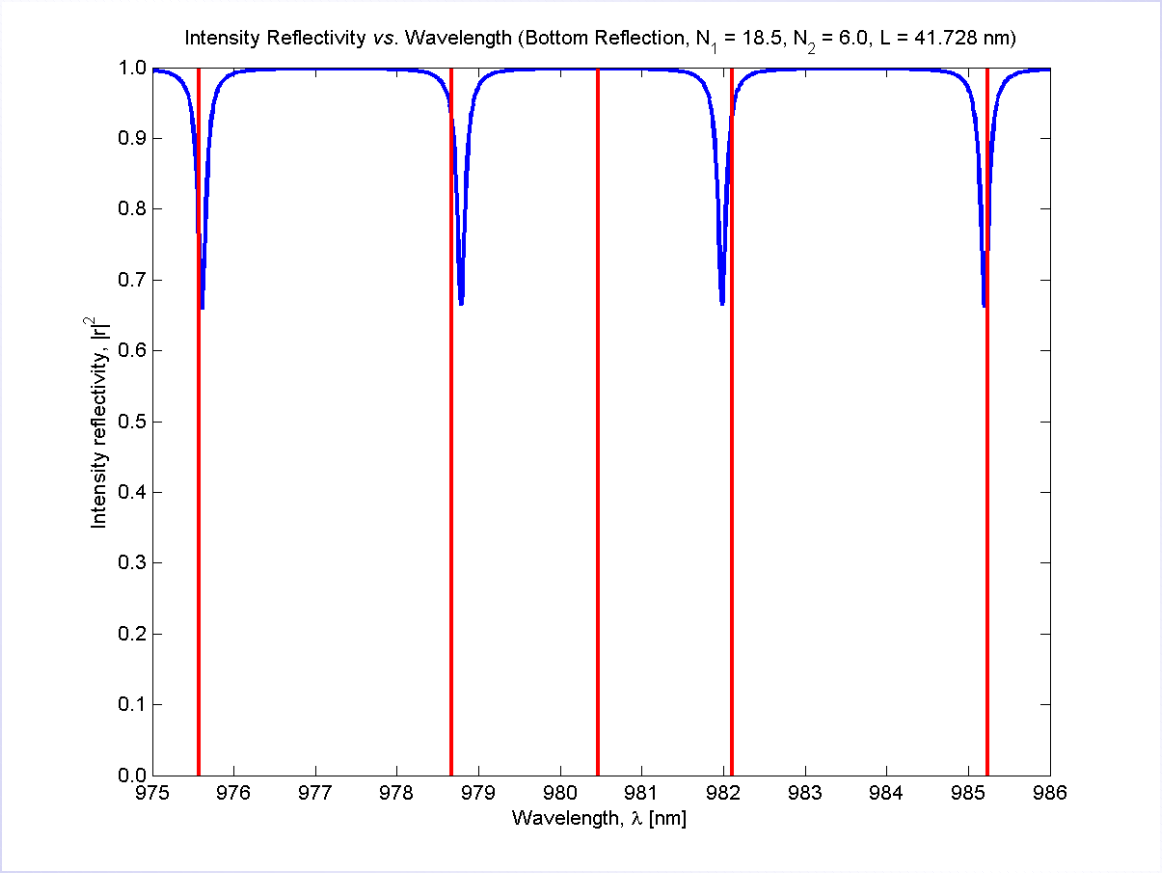
Intensity Reflectivity vs. Wavelength (Bottom Reflection, N1 = 18.5, N2 = 6.0, L = 41.728 nm)
Intensity reflectivity, |r|2
Wavelength, λ [nm]
1.0
0.9
0.8
0.7
0.6
0.5
0.4
0.3
0.2
0.1
0.0
975
976
977
978
979
980
981
982
983
984
985
986

3-Dimensional Analysis of the Benchmark CCBE-VCSEL Structure

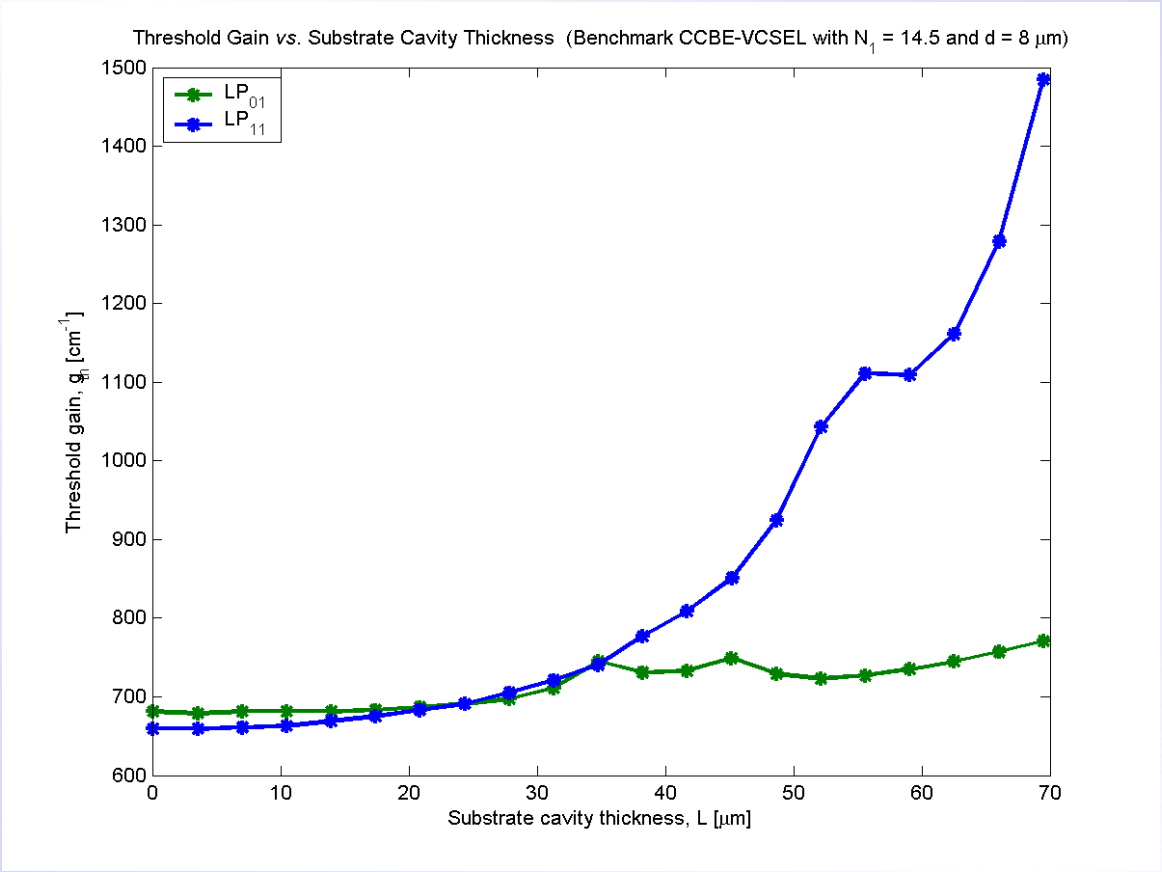
Threshold Gain vs. Substrate Cavity Thickness (Benchmark CCBE-VCSEL with N1 = 14.5 and d = 8 μm)
LP01
LP11
Threshold gain, gth [cm-1]
Substrate cavity thickness, L [μm]
1500
1400
1300
1200
1100
1000
900
800
700
600
0
10
20
30
40
50
60
70

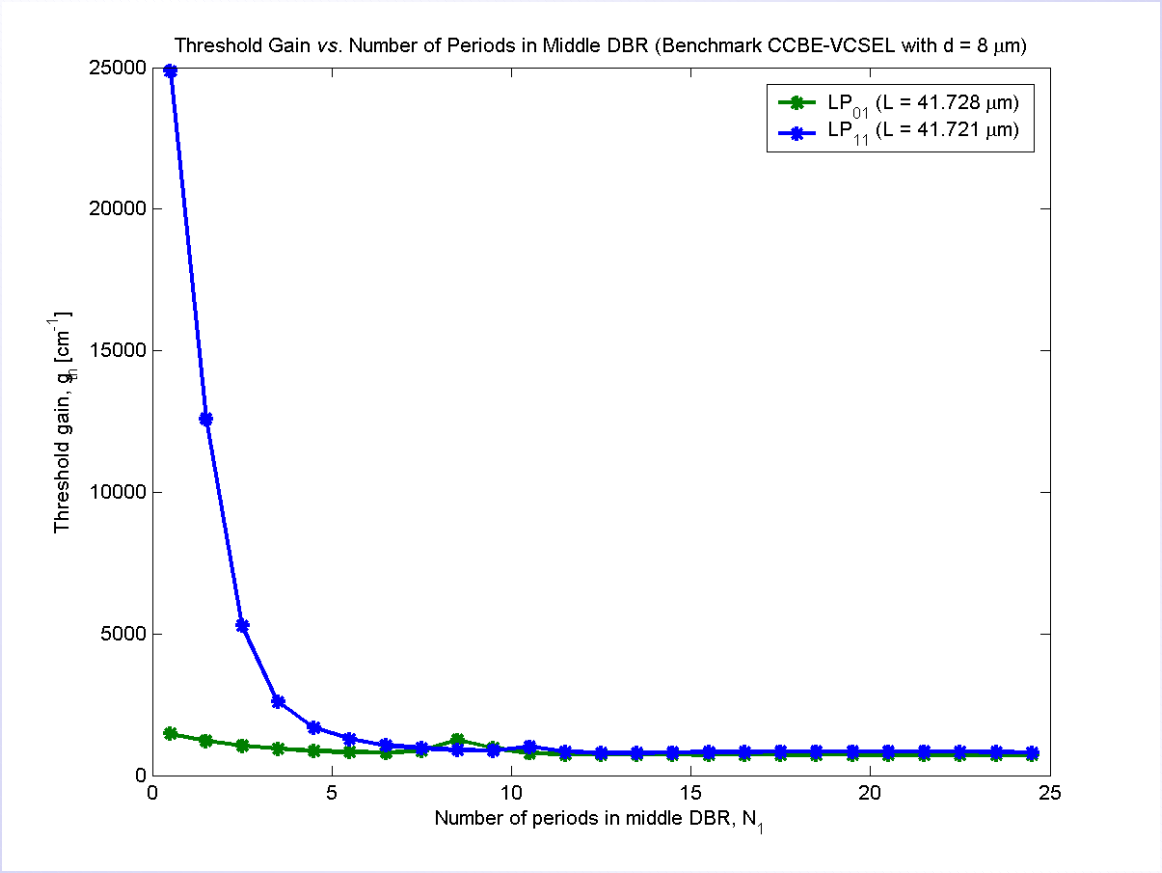
Threshold Gain vs. Number of Periods in Middle DBR (Benchmark CCBE-VCSEL with d = 8 μm)
LP01 (L = 41.728 μm)
LP11 (L = 41.721 μm)
Threshold gain, gth [cm-1]
Number of periods in middle DBR, N1
0
5000
10000
15000
20000
25000
0
5
10
15
20
25

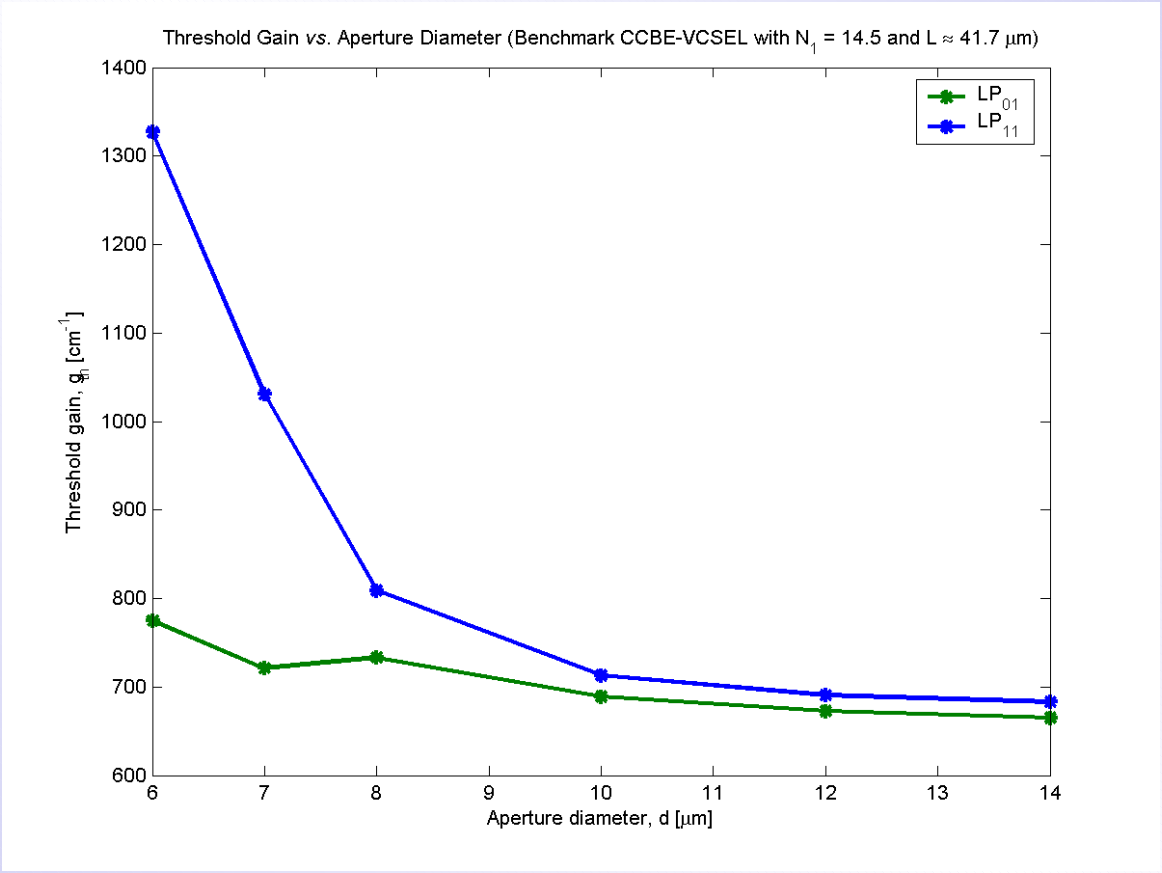
Threshold Gain vs. Aperture Diameter (Benchmark CCBE-VCSEL with N1 = 14.5 and L ≈ 41.7 μm)
LP01
LP11
Threshold gain, gth [cm-1]
Aperture diameter, d [μm]
1400
1300
1200
1100
1000
900
800
700
600
6
7
8
9
10
11
12
13
14

Conclusions and Perspectives

Conclusions

- The 1- and 3-dimensional optical field models appear to provide correct predictions for the resonance wavelengths and threshold gains of CCBE-VCSELs.
- Longitudinal- and transverse-single-mode operation of CCBE-VCSELs at high optical output powers may be possible.

Perspectives

- The complex reflection from the "bottom mirror" should be investigated further.
- The substrate cavity fine structure should be investigated further.
- A plotting routine, capable of plotting the transverse optical field distribution in the different epitaxial layers *and* outside the CCBE-VCSEL, should be implemented.
- The boundary conditions at the perimeter of the reference cylinder should be exchanged with more advanced boundary conditions.
- More complex reflection schemes at the output interface of the CCBE-VCSEL should be investigated (*e.g.* dielectric mirror, photonic gratings).

Questions?

Thank You for Listening

- Thesis and presentation at `http://master.mortenstilling.dk`
- E-mail me at `mortenstilling@mortenstilling.dk`